experiment, we anticipate that the qualitative pictures deduced from the present calculations will remain true in far more elaborate (and more computationally demanding) ab initio model Hamiltonians.

The present results show that intermolecular, chromophore–chromophore interactions can represent a major factor in determining the macroscopic second-order susceptibility of molecule-based NLO materials. The NLO response depends critically not only on the molecular packing geometries, but also significantly on the characteristics of the molecular constituents. At equilibrium chromophore–chromophore separations, the NLO response is a strong function of the relative molecular orientations. However, for relatively large intermolecular distances, particularly for component molecules having small ground-state dipole moments, each molecule may be considered to be independent of the surrounding ones, giving an additive contribution to the macroscopic susceptibility. Such effects find experimental counterparts in self-assembled or Langmuir–Blodgett thin films characterized by relatively low packing densities.[32,33] Thus, the optimization of packing density is clearly crucial for obtaining high-efficient SHG materials.

From the present results it can also be inferred that a bulk material having slipped (C_x) chromophore components would be expected to exhibit an optimum second-order nonlinearity. As a confirmatory example, 3-methyl-4-methoxy-4′-nitrostilbene (NMONS), the crystal structure of which consists of stacked π–π planar molecules in a slipped cofacial donor–acceptor (C_x-like) configuration (Figure 1), has one of the largest powder SHG efficiencies reported to date (1250 times more efficient than the urea).[34] High SHG signals are also observed from other substituted 4′-nitrostilbene derivatives which are stacked in a similar fashion,[35] and for the *N*-(4-nitrophenyl)-(L)-prolinol (NPP), the crystal structure of which consists of nearly planar molecules, in a C_x-like donor–acceptor configuration, connected by an infinite network of hydrogen-bonded chains.[36] In these cases, favorable angles between molecular charge-transfer axes (or favorable dipolar orientations within the unit cell)[8] also render these crystals well suited for efficient phase-matching.[35,36]

Finally, the two-level model, extensively used for the qualitative prediction of molecular hyperpolarizabilities, is not of general validity for calculations on chromophore clusters. In fact, for large chromophore–chromophore distances, it overestimates β. At normal chromophore–chromophore equilibrium distances, the two-level model is still valid; however, in the case of strongly delocalized intermolecular interactions, it also fails to reliably predict the hyperpolarizability.

Acknowledgments. This research was supported by the NSF-MRL program through the Material Research Center of Northwestern University (Grant DMR8821571) and by the Air Force Office of Scientific Research (Contract 90-0071). S.D.B. thanks the Italian Consiglio Nazionale delle Ricerche (CNR, Rome) for a postdoctoral fellowship. We thank Professor M. C. Zerner for providing us with the ZINDO code and Dr. D. R. Kanis for numerous helpful discussions.

Registry No. 1, 100-01-6; **2**, 1074-98-2.

(33) A recent study (Itoh, Y.; Hamada, T.; Kakta, A.; Muko, A. *SPIE Proc.* **1990**, *1337*, 293) presents some important but preliminary β results for 4-nitro-3-methylaniline in an ab initio calculation. Their results are in good qualitative agreement with ours.

(34) (a) Tam, W.; Guerin, B.; Calabrese, J. C.; Stevenson, S. H. *Chem. Phys. Lett.* **1989**, *154*, 93. (b) Bierlein, J. D.; Cheng, L. K.; Wang, Y.; Tam, W. *Appl. Phys. Lett.* **1990**, *56*, 423.

(35) Grubbs, B. R.; Marder, S. R.; Perry, J. W. *Chem. Mat.* **1991**, *3*, 3.

(36) Zyss, J.; Nicould, J. F.; Coquillay, M. *J. Chem. Phys.* **1984**, *81*, 4160.

Energetics, Proton Transfer Rates, and Kinetic Isotope Effects in Bent Hydrogen Bonds

Xiaofeng Duan and Steve Scheiner*

Contribution from the Department of Chemistry and Biochemistry, Southern Illinois University, Carbondale, Illinois 62901. *Received January 6, 1992*

Abstract: N—H···N H-bonds which occur in intermolecular contacts and in intramolecular situations where the bond is bent are investigated by ab initio methods. Distortion of the θ(N—H···N) angle of up to 40° from linearity results in modest increases in the barrier to proton transfer while a much higher barrier occurs in $NH_2CH_2NH_3^+$ where this angular distortion is some 100°. The rate of transfer is orders of magnitude slower in the latter system. In contrast to earlier suppositions that systems containing nonlinear H-bonds are subject to smaller kinetic isotope effects, k_H/k_D for the most highly strained system is larger than in the other complexes. This distinction is attributed in part to the difference in zero-point vibrational energies but primarily to the contribution of tunneling. Not only the value of k_H/k_D but also the temperature sensitivity of this parameter is enhanced by nonlinearity of the H-bond.

Introduction

Decades of experimental study of the proton transfer reaction in solution have yielded a rich harvest of information concerning mechanisms, reaction rates, and sensitivity of pK to solvent type.[1,2] More recent developments in techniques have permitted the reaction to be studied in the gas phase, free of the many complicating effects of a bulk-phase solvated environment.[3-7] It is also possible in this manner to separate the energetic and entropic factors involved in the reaction of each pair of molecules. Details about the molecular geometry associated with proton transfer have been harder to come by. Microwave measurements in the gas phase

(1) Caldin, E. F.; Gold, V. *Proton Transfer Reactions*; Halsted: New York, 1975.

(2) Stewart, R. *The Proton: Applications to Organic Chemistry*; Academic: Orlando, 1985.

(3) Cheshnovsky, O.; Leutwyler, S. *J. Chem. Phys.* **1988**, *88*, 4127. Knochenmuss, R.; Cheshnovsky, O.; Leutwyler, S. *Chem. Phys.* **1988**, *144*, 317.

(4) Dodd, J. A.; Baer, S.; Moylan, C. R.; Brauman, J. I. *J. Am. Chem. Soc.* **1991**, *113*, 5942.

(5) Meot-Ner, M.; Smith, S. C. *J. Am. Chem. Soc.* **1991**, *113*, 862.

(6) Meot-Ner, M. *J. Am. Chem. Soc.* **1989**, *111*, 2830-2834.

(7) Hierl, P. M.; Ahrens, A. F.; Henchman, M.; Viggiano, A. A.; Paulson, J. F.; Clary, D. C. *J. Am. Chem. Soc.* **1986**, *108*, 3140.

0002-7863/92/1514-5849$03.00/0

have offered useful information in a few limited cases.[8,9] Solution-phase work can provide valuable information for intramolecular H-bonds with well-defined geometries.[10-13] Structural data are forthcoming from diffraction studies of the solid state, but again, one is faced with perturbations from the surroundings.[14-16]

One of the strengths of ab initio molecular orbital theoretical methods is their ability to locate minima and other stationary points on a potential energy surface. Optimizations lead to high-precision elucidations of the molecular geometries of these minima. Unlike experimental techniques where the transient nature of transition states presents a formidable obstacle, quantum mechanical procedures are not hampered at all by this ultrashort lifetime. It is hence possible to derive the potential energy surface for a proton transfer reaction, including the H-bond geometries in both wells and the transfer transition state. Such a surface can then be used to compute the kinetics of the process.

Ab initio computations of proton transfers from one molecule to another[17-23] have established that the barrier rises quickly as the distance between the donor and acceptor atoms is stretched. Angular deformations have been shown to influence the barrier as well. Consideration of systematic variations in these geometrical parameters has facilitated extraction of a set of rules relating transfer energetics to details of H-bond geometry.

However, unlike intermolecular H-bonds where the two subunits are free to adopt their most favored relative spatial relationships, the structural constraints of the entire molecule can prevent formation of energetically favorable short, linear intramolecular H-bonds. Proton transfers have been studied in a number of molecules containing intramolecular OH···O H-bonds such as oxalic acid[24] and its deprotonated anion,[25,26] glycolate anion,[26] malonaldehyde,[27,28] hydrogen maleate,[29,30] and hydrogen malonate.[30,31] Analogous computations have been carried out for nitrogen analogues such as protonated ethylenediamine.[32] Lack

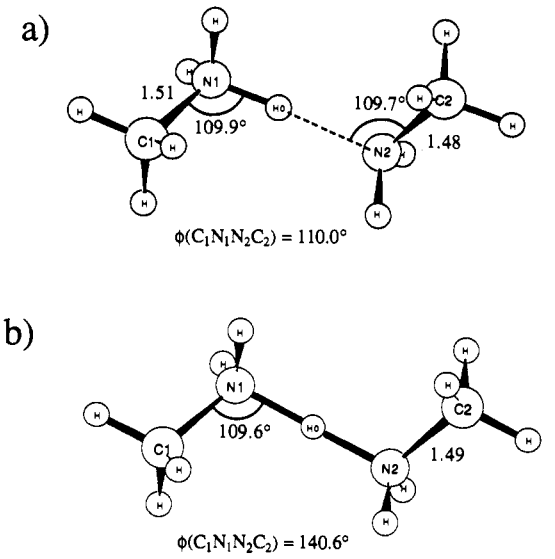

Figure 1. Geometries of (a) equilibrium and (b) transition state (C_2 point group) for proton transfer in system I. Distances shown are in Å.

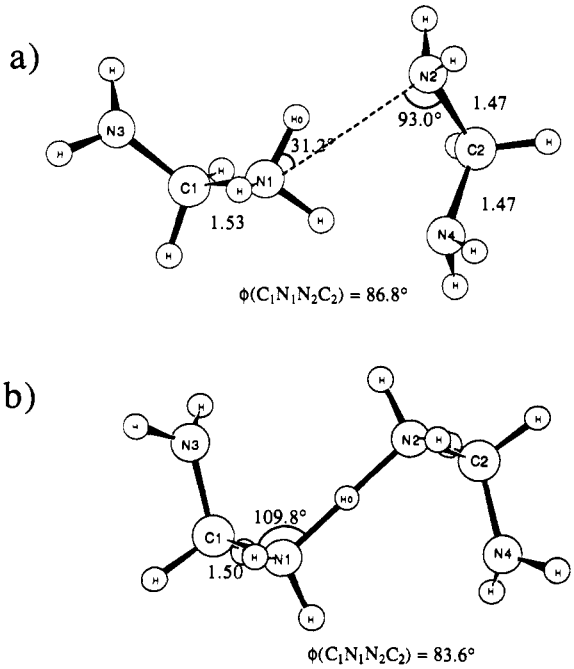

Figure 2. Geometries of (a) equilibrium and (b) transition state (C_2 point group) for proton transfer in system II. The $r(N_1N_2)$ and $r(N_1N_4)$ distances are 2.89 and 2.83 Å, respectively, in bifurcated geometry a.

of consistency within this body of data prevents extraction of systematic relationships between the H-bond geometry and the energetics of proton transfer. For example, each system was considered with a different basis set. For optimal comparison of two systems, it is preferable that all aspects of the pair be similar or identical, so as to enable focusing on the geometry of the H-bond. However, some of the previously studied systems containing an intramolecular H-bond are neutral while others are anionic; pairs also differ in the hybridization or bonding pattern of the donor and acceptor atoms.

In an effort to systematize the patterns in intramolecular H-bonds, we consider here the NH···N interactions that occur in $NH_2(CH_2)_nNH_3^+$ where n = 1, 2, 3. Each progressive addition of a CH_2 group enlarges the ring by one atom and alters the equilibrium structure and flexibility of the H-bond. But the methylene addition does not affect the bonding pattern of the

(8) Firth, D. W.; Beyer, K.; Dvorak, M. A.; Reeve, S. W.; Grushow, A.; Leopold, K. R. *J. Chem. Phys.* **1991**, *94*, 1812–1819.

(9) Baughcum, S. L.; Smith, Z.; Wilson, E. B.; Duerst, R. W. *J. Am. Chem. Soc.* **1984**, *106*, 2260–2265.

(10) Menger, F. M.; Chow, J. F.; Kaiserman, H.; Vasquez, P. C. *J. Am. Chem. Soc.* **1983**, *105*, 4996–5002.

(11) Houriet, R.; Rüfenacht, H.; Carrupt, P.-A.; Vogel, P.; Tichy, M. *J. Am. Chem. Soc.* **1983**, *105*, 3417.

(12) Alder, R. W.; Moss, R. E.; Sessions, R. B. *J. Chem. Soc., Chem. Commun.* **1983**, *1000*. Alder, R. W.; Orpen, A. G.; Sessions, R. B. *J. Chem. Soc., Chem. Commun.* **1983**, 999.

(13) Rospenk, M.; Zeegers-Huyskens, Th. *J. Phys. Chem.* **1987**, *91*, 3974.

(14) Stankowski, J.; Mackowiak, M.; Koziol, P.; Jadzyn, J. *J. Chem. Phys.* **1985**, *89*, 3188.

(15) Küppers, H.; Takusagawa, F.; Koetzle, T. F. *J. Chem. Phys.* **1985**, *82*, 5636.

(16) Fillaux, F.; Lautie, A.; Tomkinson, J.; Kearley, G. J. *Chem. Phys.* **1991**, *154*, 135.

(17) Scheiner, S. *Acc. Chem. Res.* **1985**, *18*, 174.

(18) Scheiner, S. *J. Am. Chem. Soc.* **1981**, *103*, 315.

(19) Hillenbrand, E. A.; Scheiner, S. *J. Am. Chem. Soc.* **1984**, *106*, 6266.

(20) Hillenbrand, E. A.; Scheiner, S. *J. Am. Chem. Soc.* **1985**, *107*, 7690.

(21) Hillenbrand, E. A.; Scheiner, S. *J. Am. Chem. Soc.* **1986**, *108*, 717.

(22) Cybulski, S. M.; Scheiner, S. *J. Am. Chem. Soc.* **1989**, *111*, 23.

(23) Scheiner, S. *J. Mol. Struct. (Theochem)* **1988**, *177*, 79.

(24) Bock, C. W.; Redington, R. L. *J. Chem. Phys.* **1986**, *85*, 5391.

(25) Truong, T. N.; McCammon, J. A. *J. Am. Chem. Soc.* **1991**, *113*, 7504.

(26) Bosch, E.; Moreno, M.; Lluch, J. M.; Bertran, J. *Chem. Phys.* **1990**, *148*, 77.

(27) Frisch, M. J.; Scheiner, A. C.; Schaefer, H. F., III; Binkley, J. S. *J. Chem. Phys.* **1985**, *82*, 4194.

(28) Shida, N.; Barbara, P. F.; Almlöf, J. E. *J. Chem. Phys.* **1989**, *91*, 4061.

(29) George, P.; Bock, C. W.; Trachtman, M. *J. Phys. Chem.* **1983**, *87*, 1839.

(30) Hodoscek, M.; Hadzi, D. *J. Mol. Struct. (Theochem)* **1990**, *209*, 411.

(31) Hodoscek, M.; Hadzi, D. *J. Mol. Struct. (Theochem)* **1990**, *209*, 421.

(32) Ikuta, S.; Nomura, O. *J. Mol. Struct. (Theochem)* **1987**, *152*, 315.

Table I. Geometrical Parameters and Energetics of the Equilibrium and Proton Transfer Transition State Structures

	I	II	III	IV	V
$\theta(N-H-N)^{eq}$, deg	180	134 (180)[a]	81	125	149
$\theta(N-H-N)^{ts}$, deg	180	180	111	138	157
$R(N-N)^{eq}$, Å	2.74	2.88 (2.79)	2.44	2.64	2.69
$R(N-N)^{ts}$, Å	2.59	2.58	2.19	2.42	2.52
$R^{eq} - R^{ts}$, Å	0.15	0.30 (0.21)	0.25	0.22	0.17
$r(N-H)^{eq}$, Å	1.077	1.019 (1.052)	1.009	1.030	1.053
$r(N-H)^{ts}$, Å	1.295	1.290	1.328	1.295	1.287
$E^{\dagger}$, kcal/mol	2.14	5.68 (4.60)	32.45	6.74	3.38
$E^{\dagger}$ + ΔZPE, kcal/mol	−0.33	2.76	29.65	4.19	0.79
$E^{\dagger}$(6-31G*), kcal/mol	4.32	9.07	33.67	10.61	6.25

[a] Values obtained holding $\theta(N-H-N) = 180°$ in equilibrium structure shown in parentheses.

molecule, nor does the transfer of the proton from one N atom to the other cause a rearrangement of bonds or deviation from the sp^3 hybridization of the N and C atoms. Closely related intermolecular H-bonds are also considered where there is no external strain imposed on the NH···N H-bond. Comparison with the intramolecular bonds permits unambiguous identification of the effects of the geometrical constraints upon the proton transfer properties.

There has been extensive discussion in the literature concerning the effect of nonlinearity of the transition state upon the rate of the chemical reaction or the magnitude of its kinetic isotope effect.[33-38] Examination of this series of molecules, containing unstrained intermolecular H-bonds as well as intramolecular bonds with varying degrees of strain, permits a clear correlation to be drawn between geometric aspects of the equilibrium or transition state structure and the kinetics of proton transfer.

Geometries and Energetics

A. Methods. Ab initio calculations were carried out using the 4-31G basis set[39a] within the context of the Gaussian 88 program.[40] Evidence from prior work indicates that little improvement is expected in H-bond geometries or in computed barrier heights from use of larger basis sets.[30,31] Nonetheless, these barriers were recomputed with the polarized 6-31G* basis set[39b] as well for purposes of comparison. The geometries of each complex and transition state were fully optimized using the gradient procedures contained therein. Vibrational frequencies were obtained using the harmonic approximation. The energy barriers for proton transfer are computed as the difference in SCF energy between each complex and its corresponding transition state. The complexation energies of the bimolecular $(CH_3NH_2)_2H^+$ and $(NH_2CH_2NH_2)_2H^+$ systems were taken as the difference in energy between each complex and its separated moieties, e.g. CH_3NH_2 and $CH_3NH_3^+$, each of which was fully optimized.

B. Intermolecular Transfers. The geometries of the $CH_3NH_2\cdots H^+\cdots NH_2CH_3$ (I) and $NH_2CH_2NH_2\cdots H^+\cdots NH_2CH_2NH_2$ (II) complexes are depicted in Figures 1a and 2a. Both of these complexes are fairly tightly bound; their complexation energies are 26.9 and 27.0 kcal/mol, respectively. The presence of the second nitrogen atom on the proton acceptor molecule in II leads to the possibility that two of the hydrogens on the donor can each form a H-bond. It is this dual interaction which is responsible for the nearly symmetric structure in Figure 2a wherein the $r(N_1N_2)$ and $r(N_1N_4)$ distances are 2.89 and 2.83 Å, respectively. Comparison with the structures of the isolated monomers reveals a number of perturbations occurring as a direct result of complexation. The C–N bond of CH_3NH_2 elongates by 0.034 Å in system I while that in $CH_3NH_3^+$ contracts by 0.020 Å. The bridging N–H bond stretches by 0.07 Å, characteristic of H-bond formation.

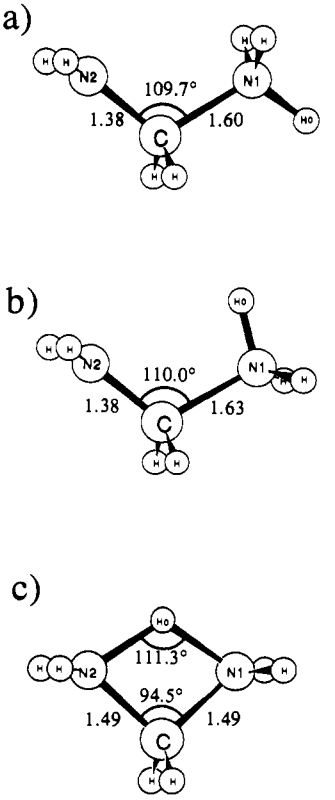

Figure 3. Geometries of (a) equilibrium and (c) transition state (C_{2v} point group) for intramolecular proton transfer in system III, $NH_2CH_2NH_3^+$. Structure b is obtained from a by rotation about the CN_1 bond axis. It is not a true minimum but is instead a transition state with respect to this rotation. In all cases, C, N_1, N_2, and H_0 lie in a common plane.

The hydrogen bond in complex I is linear; i.e. $\theta(N—H\cdots N) = 180°$. The same is true of the transition state following the half transfer of the proton, as illustrated in Figure 1. The principal geometric change occurring in the complex as a result of this half transfer is the reduction of the intermolecular $R(NN)$ separation by 0.15 Å, as listed in Table I. Although neither of the H-bonds is linear for the equilibrium structure of complex II, half transfer of one proton induces a reorientation to make this bond linear in the transition state. The intermolecular angle $\theta(N1-N2-C2)$, for example, increases from 93° to 110°, accompanied by the expected contraction of the intermolecular N–N distance, by 0.3 Å. If the H-bond in system II is forced to become linear by setting $\theta(N1—H\cdots N2) = 180°$, the energy rises by 1.1 kcal/mol relative to the lowest energy structure in Figure 2a. The geometric and energetic parameters of this complex are listed in parentheses in Table I.

The potential energy surface for proton transfer in system I is rather flat. The electronic contribution to the transfer barrier is 2.1 kcal/mol and drops to a negative value (−0.3 kcal/mol) after correction for zero-point vibrational energies. Due in part to the bifurcated equilibrium structure of system II, its transfer barrier (5.7 kcal/mol) is higher than that of system I; the potential maintains its double-well character even after zero-point energy correction. In the case where the equilibrium structure is assumed to contain a linear H-bond, the barrier is somewhat lower but still higher than that obtained for I. This higher barrier is consistent with the longer internitrogen separation in II.

C. Intramolecular Transfers. Intramolecular proton transfer between nitrogen atoms was examined for the three ions

(33) Melander, L.; Saunders, W. H., Jr. *Reaction Rates of Isotopic Molecules*; Wiley-Interscience: New York, 1980.
(34) Hawthorne, M. F.; Lewis, E. S. *J. Am. Chem. Soc.* **1958**, *80*, 4296.
(35) Bigeleisen, J.; Mayer, M. G. *J. Chem. Phys.* **1947**, *15*, 261.
(36) More O'Ferrall, R. A. *J. Chem. Soc. B* **1970**, 785.
(37) Anhede, B.; Bergmann, N.-Å. *J. Am. Chem. Soc.* **1984**, *106*, 7634.
(38) Liotta, D.; Saindane, M.; Waykole, L.; Stephens, J.; Grossman, J. *J. Am. Chem. Soc.* **1988**, *110*, 2667.
(39) (a) Ditchfield, R.; Hehre, W. J.; Pople, J. A. *J. Chem. Phys.* **1971**, *54*, 724. (b) Hariharan, P. C.; Pople, J. A. *Theor. Chim. Acta* **1973**, *28*, 213.
(40) Frisch, M. J.; Head-Gordon, M.; Schlegel, H. B.; Raghavachari, K.; Binkley, J. S.; Gonzalez, C.; DeFrees, D. J.; Fox, D. J.; Whiteside, R. A.; Seeger, R.; Melius, C. F.; Baker, J.; Martin, J.; Kahn, L. R.; Stewart, J. J. P.; Fluder, E. M.; Topiol, S.; Pople, J. A., Gaussian, Inc.: Pittsburgh, PA 1988.

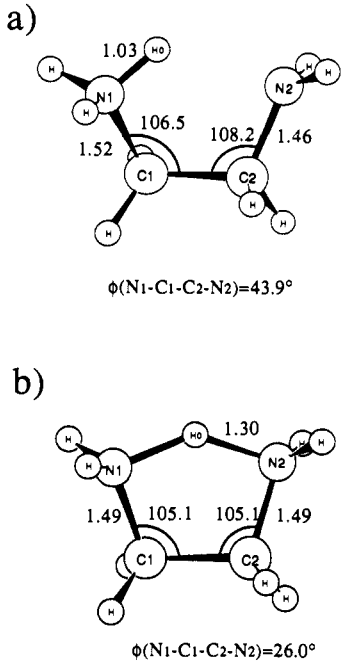

Figure 4. Geometries of (a) equilibrium and (b) transition state (C_2 point group) for intramolecular proton transfer in system IV, $NH_2CH_2CH_2NH_3^+$. The framework is not planar; dihedral angles are shown.

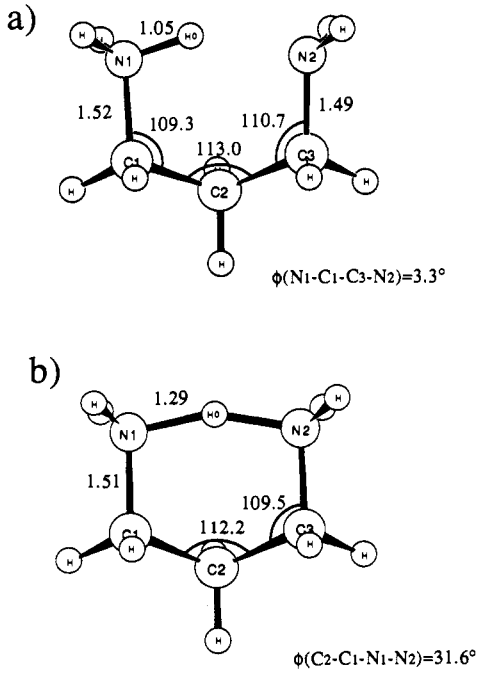

Figure 5. Geometries of (a) equilibrium and (b) transition state (C_s point group) for intramolecular proton transfer in system V, $NH_2CH_2CH_2CH_2NH_3^+$. The framework is not planar; dihedral angles are shown.

$NH_2CH_2NH_3^+$ (III), $NH_2CH_2CH_2NH_3^+$ (IV), and $NH_2CH_2CH_2CH_2NH_3^+$ (V). Their geometries and those of their proton transfer transition states are illustrated in Figures 3, 4, and 5, respectively. The salient features of the H-bond in each geometry are listed in Table I along with the transfer barriers. Because of the intramolecular nature of the H-bond, both equilibrium and transition state structures contain angular distortions of varying degree. Considering the linearity of each ion, θ(NHN) increases from 81° for III, to 125° for IV, and more nearly linear at 149° for V. This pattern is consistent with diminishing strain on the H-bond as the number of atoms in the ring increases. Indeed, there is some question as to whether a hydrogen bond exists

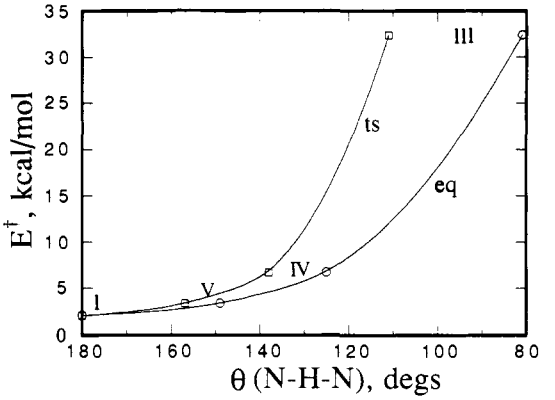

Figure 6. Proton transfer barrier $E^\dagger$ shown as a function of nonlinearity of the intramolecular H-bond in the equilibrium (eq) and transition state (ts) of various complexes. Roman numerals refer to the complex from whence data are derived. Angles are taken from the first two rows of Table I.

at all in three-membered ring III.[41] The lowest energy structure, pictured in Figure 3a, does not have a hydrogen bridging the two N nuclei. Rotation of the NH_3 group so as to form such a bridge leads to the second geometry in Figure 3b, which is a transition state on the surface (with this rotation as its reaction coordinate), 1.4 kcal/mol higher in energy than the true minimum. The proton transfer was considered from the latter structure to the structure in Figure 3c. Structure IV lessens the strain by having the two nitrogen atoms rotate out of the molecular plane; the ϕ(NCCN) torsional angle is 44° in the equilibrium structure.

Half transfer of the proton reduces some of the strain in each case as is evident by the larger values of θ(NHN) for the transition states relative to the equilibrium geometries (see Table I). As in the intermolecular cases, the internitrogen distance undergoes a shortening as the proton reaches the transfer midpoint. These reductions vary from 0.25 Å for III down to 0.17 Å for the five-membered ring. The transfer barriers diminish as the strain in the H-bond is alleviated. The barrier for the five-membered ring is comparable to those of intermolecular transfer where there is no nonlinearity at all while the highly strained three-membered ring III yields an inordinately high barrier to proton transfer. Using the semiempirical MNDO method, Anhede et al.[37] obtained a slightly more strained transition state for III, with θ(NHN) = 104°, while Menger et al.[42] found an angle of 103° using the similar MINDO/3 method.

The relationship between the strain and transfer barrier is visualized in Figure 6 which plots the barrier as a function of the nonlinearity of the H-bond in both the equilibrium and transition state geometries. That is, the θ(N–H–N) angle in the optimized equilibrium structure of each complex is compared with the calculated proton transfer barrier $E^\dagger$ in the curve labeled "eq" in Figure 6; the same barrier is plotted vs the same angle in the transition state for the "ts" curve. It appears that deviations of even up to 40–50° from linearity (180°) do not affect the barrier much, but it rises quickly as the deformation increases. The barriers are more sensitive to the nonlinearity in the transition state than in the equilibrium geometry.

Other than the geometry of the H-bond itself, there does not appear to be much strain engendered within the ring by this bond. All the bond angles centered on a C atom are within 4° of the tetrahedral angle in either the equilibrium or transition state structures.

The effects upon the barrier of enlarging the basis set may be seen in the last row of Table I which presents results obtained with the polarized 6-31G* set (with geometries optimized at the 4-31G level). As expected from earlier work[17,43] the larger basis

(41) The number of atoms contained in each ring refers in this work to the number of non-hydrogen atoms. This nomenclature maintains consistency with the numbering of systems as well.

(42) Menger, F. M.; Grossman, J.; Liotta, D. C. *J. Org. Chem.* **1983**, *48*, 905.

Table II. Imaginary Frequencies (cm^{-1}) for Proton Transfer Transition States

	I	II	III	IV	V
all-H	1206.7	1174.1	1967.5	1426.5	1323.6
mono-D	867.7	859.5	1426.1	1032.6	955.9
all-D	864.2	851.1	1423.5	1030.4	952.7

Table III. Zero-Point Vibrational Energies and Transfer Barrier (kcal/mol)

		ZPE^{eq}	ZPE^{ts}	ΔZPE	$E^{\dagger}$ + ΔZPE
I	all-H	98.14	95.67	−2.47	−0.33
	mono-D	95.88	94.19	−1.69	0.45
	all-D	73.01	71.30	−1.71	0.43
II	all-H	122.43	119.51	−2.92	2.76
	mono-D	120.06	118.06	−2.00	3.68
	all-D	92.11	90.07	−2.04	3.65
III	all-H	65.17	62.37	−2.80	29.65
	mono-D	62.81	60.94	−1.87	30.58
	all-D	48.76	46.83	−1.93	30.52
IV	all-H	85.42	82.87	−2.55	4.19
	mono-D	83.08	81.39	−1.69	5.05
	all-D	64.32	62.53	−1.79	4.95
V	all-H	104.81	102.22	−2.59	0.79
	mono-D	102.47	100.72	−1.75	1.63
	all-D	79.17	77.36	−1.81	1.58

set produces barriers higher by some 2–4 kcal/mol.

Kinetics

A. Methods. By using transition state theory, it is straightforward to input the energetics and geometries of proton transfer from the previous section, along with vibrational frequencies, and arrive at kinetic data. System I is discarded from consideration as its potential has only a single symmetric minimum following inclusion of zero-point vibrational energies. In order to estimate kinetic isotope effects, rates were computed not only for the systems discussed above but also for their fully deuterated analogs and that in which only the bridging protium is changed to D.

Because it corresponds to a reaction coordinate, the proton transfer motion leads to an imaginary frequency in each transition state. These frequencies are reported in Table II for each of the complexes. Table III reports the total zero-point vibrational energies along with the adjusted barrier for each system. Note that the singly and fully deuterated complexes have very nearly the same barrier.

Within the context of transition state theory, the kinetic isotope effect (KIE) can be partitioned as a series of ratios:[35]

$$\mathrm{KIE} = \frac{k_H}{k_D} = \frac{Q_H}{Q_D} \times \mathrm{MMI} \times \mathrm{EXC} \times \mathrm{ZPE} \qquad (1)$$

The Q ratio refers to a tunneling correction for which Wigner's expression[44] serves as a convenient starting point

$$Q = 1 + \frac{1}{24}\left[\frac{h\nu_i}{kT}\right]^2 \qquad (2)$$

where ν_i is the imaginary frequency of the transition state.

The second term in eq 1 is the mass and moment-of-inertia term. For the unimolecular reactions considered here, the masses of reactants and transition states are identical so this term reduces to

$$\mathrm{MMI} = \left(\frac{A_H^{\ddagger}B_H^{\ddagger}C_H^{\ddagger}}{A_D^{\ddagger}B_D^{\ddagger}C_D^{\ddagger}} \frac{A_DB_DC_D}{A_HB_HC_H}\right)^{1/2} \qquad (3)$$

where A and $A^{\ddagger}$ are the moments of inertia of the reactants and transition states, respectively. The EXC (excitation) term arises from any appreciable populations of vibrational states above the ground state, while the final term in eq 1 accounts for the zero-point vibrational energies.

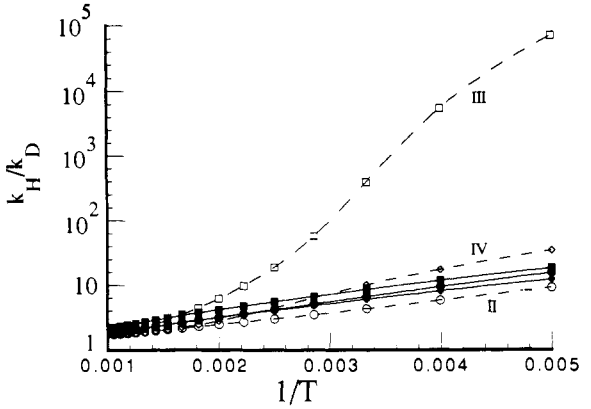

Figure 7. Kinetic isotope effect for full deuteration plotted against reciprocal temperature (K). Solid curves refer to the transition state model with tunneling incorporated by Wigner correction (eqs 1–3) and broken curves to data obtained with the RRKM approach with tunneling incorporated explicitly at each energy of the microcanonical ensemble. Circles refer to system II, squares to III, and diamonds to IV.

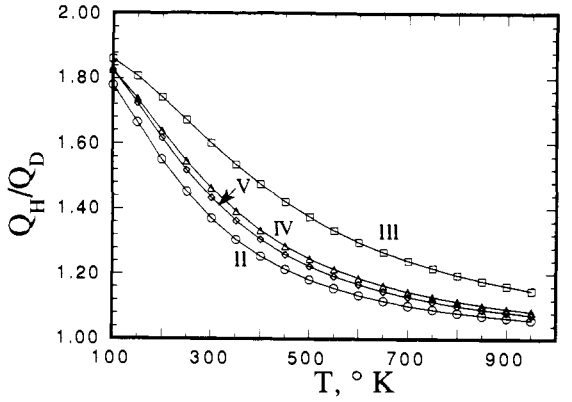

Figure 8. Plot of the contribution of Wigner tunneling to the kinetic isotope effect for full deuteration. Circles refer to system II, squares to III, diamonds to IV, and triangles to V.

B. Results. The deuterium isotope effects computed by eq 1 are illustrated as a function of reciprocal temperature by the solid curves in Figure 7 from which it may be seen that the KIE is very nearly exponential with respect to $1/T$. k_H/k_D varies from a high of about 15 when T = 200 K down to 2 when T has risen to 1000 K. The magnitude of the KIE is slightly larger for complex III than for the others at all temperatures considered.

One can analyze this behavior via the various terms in eq 1. The MMI term plays little role in the KIE since it is very nearly unity at all temperatures. In other words, the substitution of H by D has little effect upon equilibrium or transition state geometries and consequently upon their moments of inertia. Figure 8 plots the behavior of the tunneling contribution to KIE, Q_H/Q_D. Of course, as the temperature falls, tunneling plays an increasingly larger role in the transfer process so it is not surprising to see the curves rise toward the left. Nonetheless, the magnitudes of these values of Q_H/Q_D are rather small, less than 2, even down to 100 K. It is instructive to note again a larger effect for III than for the other complexes, due to the relationship between nonlinearity of the H-bond and the magnitude of the imaginary frequency. The EXC term contributes little to the kinetic isotope effect. It never exceeds 1.3, even at temperatures of 800 K where appreciable populations of excited vibrational states may be expected.

Figure 9 reveals that the largest contribution to the KIE arises from the ZPE term which reaches 6 at 250 K. This term is related to the difference between ΔZPE(H) and ΔZPE(D), where ΔZPE is the zero-point energy difference between the transition state and equilibrium geometries. The near coincidence of curves II

(43) Scheiner, S.; Szczesniak, M. M.; Bigham, L. D. *Int. J. Quantum Chem.* **1983**, *23*, 739. Latajka, Z.; Scheiner, S. *J. Mol. Struct. (Theochem)* **1991**, *234*, 373. Szczesniak, M. M.; Scheiner, S. *J. Chem. Phys.* **1982**, *77*, 4586.

(44) Wigner, E. *Z. Phys. Chem.* **1932**, *19*, 203.

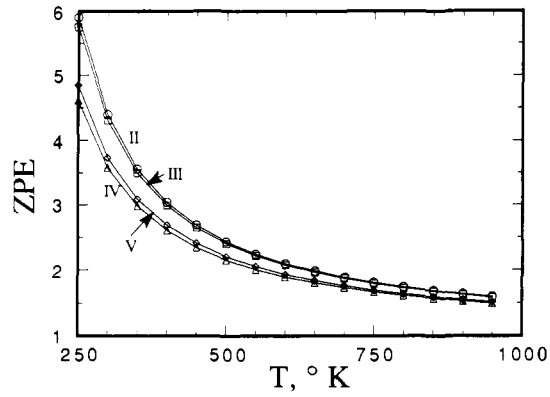

Figure 9. Plot of the contribution of zero-point vibrational energy difference to the kinetic isotope effect for full deuteration.

Table IV. Ratio of Preexponential Factors A_H/A_D and Activation Energy Difference $E_H - E_D$ (kcal/mol)

		no tunneling		with tunneling		VA/RRKM	
		A_H/A_D	$E_H - E_D$	A_H/A_D	$E_H - E_D$	A_H/A_D	$E_H - E_D$
II	all-D	1.137	0.870	1.073	1.089	1.176	0.731
	mono-D	1.097	0.773	1.036	0.988		
III	all-D	1.273	0.852	1.334	1.103	0.756	1.687
	mono-D	1.189	0.881	1.235	1.137	0.005[a]	6.63[a]
IV	all-D	1.225	0.721	1.184	0.965	1.018	0.957
	mono-D	1.167	0.813	1.124	1.058		
V	all-D	1.155	0.756	1.103	0.996		
	mono-D	1.124	0.793	1.071	1.032		

[a] Low-temperature region; all-D.

and III is a consequence of their very similar values of ΔZPE; the same is true of the IV and V curves (see Table III).

A linear fit of the Arrhenius plots in Figure 7 allows extraction of the preexponential terms A_H/A_D as well as the differences between the effective transfer barriers in the substituted and unsubstituted systems. These quantities are reported in Table IV and presented as a function of H-bond nonlinearity in Figure 10. It is readily apparent that the A_H/A_D ratio increases as the H-bond becomes less linear. In most cases, including the effects of tunneling decreases this ratio; the exception is the heavily strained system III on the far right of Figure 10.

Our results thus confirm, at least to an extent, the assumption[37] that most of the KIE originates in the ZPE term. On the other hand, there remains a significant fraction which is due to tunneling, as embodied here by Q_H/Q_D. Computation of this contribution relies on the Wigner expression which is valid only when tunneling is a minor component of the process. A more rigorous way of evaluating tunneling rests on the RRKM formalism of calculating microcanonical rate constants.[45] For energies below the top of the barrier, the tunneling transmission coefficient may be substituted for the density of states term.[46] In our calculations, the transmission coefficient is obtained by fitting the computed barrier to an Eckart potential.[46,47] Such a procedure is consistent with a vibrationally adiabatic (VA) treatment of rate computations.[48]

The rate constant ratio obtained by this more complete treatment of tunneling is presented as the series of dashed lines in Figure 7. Comparison with the solid curves reveals that for systems II and IV there is not a very large discrepancy between the results achieved by the two methods. On the other hand, the data differ dramatically in the context of system III, with its much higher barrier and more distorted H-bond. The distinctly sharper rise of the VA kinetic isotope effect as the temperature drops illustrates the inability of the Wigner correction to satisfactorily account for tunneling when this phenomenon becomes important.

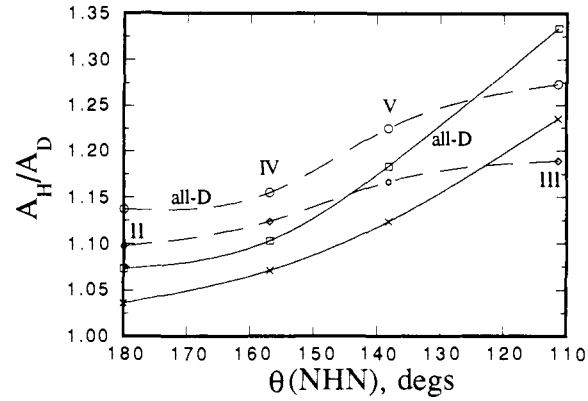

Figure 10. Plot of the isotopic ratio of preexponential factors as a function of the θ(NHN) angle in the transfer transition state. Tunneling is omitted in the broken curves. Deuteration is either only for the bridging H or for all hydrogens (as indicated). Roman numerals indicate the particular complex.

k_H/k_D reaches values exceeding 5000 as the temperature drops below 250 K. Such large isotope effects are not unexpected as they have been noted experimentally. Mordzinski for example[49] has observed KIE of several thousand in low-temperature studies of *o*-hydroxyphenylbenzooxazole while values in excess of 100 have been noted by Miyazaki et al.[50] for the proton transfer in the solid state between ethanol and benzene anion.

Linear fitting of the dashed curves in Figure 7 leads to an Arrhenius preexponential factor and isotopic energy difference for systems II, III, and IV, extracted from the VA treatment of transfer which includes tunneling explicitly. Most intriguing are the results for system III which has the highest barrier to transfer. The dashed III curve in Figure 7 is approximately bimodal in appearance. It is nearly linear in the low T range on the right as well as on the left, when $1/T < 0.002$. Both of these linear regimes were fit individually and the results are listed in Table IV. The high-temperature parameters are somewhat different than the Eyring properties. A_H/A_D is less than unity and $E_H - E_D$ is nearly 2 kcal/mol. This difference is greatly enhanced in the low-temperature region where tunneling appears to dominate the entire process. As a result, A_H/A_D drops by several orders of magnitude while the VA barrier difference becomes larger than 6 kcal/mol.

Discussion

The data reveal that angular strain on the N—H···N hydrogen bond causes the energy barrier for proton transfer to increase. The weakening of the covalent N—H bond in the transition state to transfer permits the proton to more closely approach the N···N axis and relieve a bit of the strain which is present in the equilibrium geometry. Since the strain diminishes as the number of atoms in the molecular framework increases, the barriers are lowered for the larger systems considered here. These larger molecules contain a longer N—H···N distance which normally is associated with higher barriers[17-22] so the effects of angular strain clearly outweigh the distance factor. The larger molecules also exhibit lesser change in the geometry of the H-bond as a result of half proton transfer. For example, the highly strained system $NH_2CH_2NH_3^+$ undergoes a change of 30° in θ(N—H···N) and a reduction of 0.25 Å in R(N···N). These values compare with only 8° and 0.07 Å for $NH_2CH_2CH_2CH_2NH_3^+$.

Angular distortions from linearity in the H-bond of 30–40° can be easily tolerated without substantially reducing the transfer rate, as supposed by Menger.[51] MINDO/3 calculations[42] found some flexibility in the position of the bridging proton in the transition state of $NH_2CH_2NH_3^+$. In our own ab initio calculations, it is

(45) Robinson, P. J.; Holbrook, K. A. *Unimolecular Reactions*; Wiley-Interscience: New York, 1972. Forst, W. *Theory of Unimolecular Reactions*; Academic: New York, 1973.
(46) Miller, W. H. *J. Am. Chem. Soc.* **1979**, *101*, 6810.
(47) Scheiner, S.; Latajka, Z. *J. Phys. Chem.* **1987**, *91*, 724.
(48) Truhlar, D. G.; Kuppermann, A. *J. Am. Chem. Soc.* **1971**, *93*, 1840.
(49) Mordzinski, A. J. Dissertation, Polish Academy of Sciences, Warsaw, Poland, 1990.
(50) Miyazaki, T.; Shiba, T.; Fueki, K.; Kamiya, Y. *J. Phys. Chem.* **1991**, *95*, 9115.
(51) Menger, F. M. *Tetrahedron* **1983**, *39*, 1013.

only for $NH_2CH_2NH_3^+$ with its highly distorted geometry wherein the equilibrium and transition state values of θ(N—H···N) are 81° and 111°, respectively, that the barrier rises dramatically and there is a precipitate falloff in transfer rate.

Rates of proton transfer are inversely, and very strongly, related to barrier height. For example, the rate constant of $NH_2CH_2NH_3^+$, with its barrier of 32 kcal/mol, is calculated to be some 15 orders of magnitude smaller than that for $NH_2CH_2CH_2NH_3^+$, with a barrier height of 7 kcal/mol, at 300 K. What is perhaps more interesting are deuterium isotope effects as these are used for diagnostic purposes to deduce the mechanism of various reactions. All systems show a diminishing KIE as the temperature climbs. When the rate is calculated by the vibrationally adiabatic method, ln (k_H/k_D) is quite nearly linear with respect to the reciprocal temperature. The curves for the various complexes are approximately parallel to one another, despite widely varying degrees of strain in the H-bond. Similar parallel behavior was noted earlier by Dormans and Buck[52] in their study of the [1,5]-H shift in *cis*-1,3-pentadiene. A more empirical study of the same system found temperature sensitivity of the KIE for all angles examined between 90° and 180°.[53] In agreement with Anhede and Bergman,[37] this finding belies the notion in the literature that nonlinearity of the transition state endows the KIE with temperature insensitivity.[54,55]

At any temperature, the KIE associated with the strained intramolecular H-bond in $NH_2CH_2NH_3^+$ is larger than that of the other complexes with lower barriers by a factor of 1.4 or so. At 300 K for example, the KIE for $NH_2CH_2NH_3^+$ is about 8 as compared to 5 for the other three complexes. A small part of this difference resides in the (Wigner) tunneling, and most of the remainder is due to the difference in zero-point vibrational energy. Similar conclusions, albeit very different numerical values, are arrived at when the rates are computed using the VA formalism. In this case, k_H/k_D is quite a bit larger for $NH_2CH_2NH_3^+$, especially at lower temperatures. Taking 300 K as an example once again, the KIE for $NH_2CH_2NH_3^+$ is 400 as compared to 4–10 for the other two, less strained, complexes. This much larger discrepancy is an indication of the greater role played by tunneling than can be accommodated by the Wigner correction which is really only appropriate when tunneling is of minor consequence.

It is commonly expected that bent transition states should be associated with smaller deuterium isotope effects.[33,34] This presumption is based largely on highly idealized models.[36] Liotta et al.[38] had observed a reduction in isotope effect as the transition state for proton transfer during furan metalation becomes distorted. It is difficult to compare this result with the data presented here, however, since their system does not contain a H-bond in the equilibrium geometry and appears to be complicated by a concerted transfer of another atom. On the basis of a number of poorly justified assumptions about the various vibrational frequencies, Anhede and Bergman[37] concurred that a weaker KIE should be associated with a nonlinear H-bond. Their MNDO results suggested the KIE for the strained H-bond of $NH_2CH_2NH_3^+$ is smaller by a factor of 1.3 than that in our system II, which contains an intermolecular H-bond, in direct contrast to our own finding that more strained systems have a larger KIE. Part of this discrepancy arises from their failure to include any account whatsoever of tunneling which tends to preferentially enlarge the kinetic isotope effect of the strained H-bond (see above). This trend of a larger KIE for the strained intramolecular H-bond is valid whether the rates are calculated by transition state theory with Wigner tunneling or via the vibrationally adiabatic approach. Our contention is supported by the theoretical analysis of hydride transfer by Jones and Urbauer,[56] who noted a small KIE for a linear transition state. The good agreement of their data with experiment lends further credence to this conclusion. Dormans and Buck[52] also found a smaller KIE for the transition state which contained a more linear C···H···C arrangement.

An argument presented for reduction of isotope effects as the transition state becomes more bent rests on the notion that a linear H-bond contains a relatively pure N–H stretch which becomes contaminated with bending elements as the geometry is distorted. Since the N–H stretching frequency should be reduced more by deuteration than a bending mode,[38] the vibrational energy of the linear H-bond will be lowered more upon deuteration, i.e. be subject to larger KIE. However, this idea presupposes the existence of such a pure stretching mode in these complexes, one uncontaminated by other degrees of freedom. Analysis of the normal vibrational modes of the various systems indicates the absence of such a mode. There is some degree of N–H stretching character in a number of different modes of the equilibrium geometries of the H-bonded rings, making it difficult to assign one in particular as that vibration which describes the proper motion of the proton to be transferred. Making an educated guess as to which mode is best described in this way, the vibrational frequencies are computed to be 1260, 1228, and 1284 cm^{-1} for the three-, four-, and five-membered rings, respectively. Thus the high degree of strain contained within the smallest ring is not reflected in these frequencies at all. Deuteration of the bridging hydrogen leads to reduction of these frequencies by 297, 129, and 202 cm^{-1}, respectively, again not in accord with expectations of the smallest effect in the most highly strained system. It should be stressed that even complex I, with its fully linear H-bond, does not contain a normal mode which corresponds to a pure N–H stretch of the sort employed in the simple arguments advanced previously.

Failing to confirm the ideas based upon a single N–H stretch, we turn then to consideration of all the vibrational modes together. Complex I is of intermolecular type and contains a fully linear H-bond while there is a highly distorted single H-bond in III. Contrary to the expectation of a larger effect for a linear H-bond, Table III reveals that monodeuteration lowers the total zero-point vibrational energy of the equilibrium structure of complex I by 2.26 kcal/mol, 0.1 *less* than the reduction in the energy of III. Moreover, the deuteration-induced energy lowering of complex II, with its bifurcated intermolecular H-bond, is identical with that of III. Despite significant differences in strain, the vibrational energies of the three-, four-, and five-membered rings are all lowered by the same amount upon deuteration of the bridging hydrogen. Nor do the deuteration-induced vibrational energy lowerings of the five transition states to proton transfer exhibit any significant differences from one complex to the next. There is thus no confirmation found here at all for the notion that the susceptibility of the total vibrational energy of the system to deuteration is sensitive to the degree of nonlinearity of the H-bond.

In a broader sense, one can conceptually increase the nonlinearity to the point of extinguishing the H-bond entirely. It would not be unexpected to observe larger isotope effects here since it is the H-bond which leads to a "looser" environment for the bridging hydrogen and attendant reduction of isotope effects.[57]

Tunneling is suspected of lowering the A_H/A_D ratios and of increasing the apparent activation energy difference between protiated and deuterated complexes. These expectations are for the most part confirmed by inspection of Table IV. For example, A_H/A_D for system II is reduced from 1.137 to 1.073 when (Wigner) tunneling is included and the $E_H - E_D$ difference rises from 0.87 to 1.09 kcal/mol. The only exception to this rule is A_H/A_D for highly strained $NH_2CH_2NH_3^+$ which undergoes a small rise upon deuteration. These deuteration-induced changes are more pronounced when tunneling is computed more explicitly via the VA method. In particular, A_H/A_D for system III drops down to 0.005 at low temperature while $E_H - E_D$ climbs up to 6.6 kcal/mol, six times larger than its magnitude with tunneling excluded. Changes of comparable magnitude have been noted in experimental situations in the past.[58]

(52) Dormans, G. J. M.; Buck, H. M. *J. Am. Chem. Soc.* **1986**, *108*, 3253.
(53) McLennan, D. J.; Gill, P. M. W. *J. Am. Chem. Soc.* **1985**, *107*, 2971.
(54) Kwart, H.; Gaffney, A. H.; Wilk, K. A. *J. Chem. Soc., Perkin Trans.* **1984**, *2*, 565.
(55) Kwart, H.; Wilk, K. A.; Chatellier, D. *J. Org. Chem.* **1983**, *48*, 756.
(56) Jones, J. P.; Urbauer, J. L. *J. Comput. Chem.* **1991**, *12*, 1134.
(57) Kreevoy, M. M.; Liang, T. M. *J. Am. Chem. Soc.* **1980**, *102*, 3315.
(58) Fujisaki, N.; Ruf, A.; Gäumann, T. *J. Phys. Chem.* **1987**, *91*, 1602.

Caldwell et al.[59] noted a surprisingly large deuterium isotope effect of approximately 2 for the cis-trans isomerization of 1-phenylcyclohexene. The authors found little evidence of tunneling and attributed the bulk of this large effect to zero-point vibrations. Other workers[60] found much smaller isotope effects, barely larger than unity, in bond rotation of formamide and moreover ascribed most of this effect to excitation terms. We have examined this question for the C-N bond rotation that converts our complex IIIa to IIIb and find a situation intermediate between these two extremes. Restricting our discussion first to 300 K, we find that replacement of a single H atom of the NH_3 group by D leads to a value for k_H/k_D of 1.11 whereas full deuteration of all hydrogens yields a larger value of 1.36. In either case, both ZPE and EXC make comparable contributions to the total. Tunneling, as estimated by the Wigner correction, is negligible at 300 K. As the temperature is reduced, k_H/k_D increases; ZPE becomes progressively more dominant and EXC less so. Taking 75 K as an example, the KIE is equal to 1.19 for the singly deuterated case and 1.45 for the fully deuterated case. In either case, this value is comprised almost exclusively of ZPE. Wigner tunneling raises both quantities significantly at this lower temperature, to 1.26 and 1.71, respectively. Raising the temperature above 300 K has an opposite effect in that the full k_H/k_D continues to diminish and EXC becomes the sole contributor.

In summary, distorted H-bonds lead to nonlinear transition states. A certain amount of angular strain is allowed before the barrier rises much. The higher barriers are responsible for greatly slowed proton transfer and for larger kinetic isotope effects. There is no justification found for the notion that isotope effects of nonlinear transition states are less pronounced or suffer from reduced sensitivity to temperature.

Acknowledgment. The authors are grateful to Prof. A. J. Kresge for bringing to our attention the issue raised by Caldwell et al. and for providing his own preliminary data. This research was supported financially by the National Institutes of Health (GM29391).

Registry No. $NH_2CH_2NH_3^+$, 62901-70-6; $NH_2(CH_2)_2NH_3^+$, 26265-69-0; $NH_2(CH_2)_3NH_3^+$, 26265-70-3; $CH_3NH_3^+$, 17000-00-9; D_2, 7782-39-0.

(59) Caldwell, R. A.; Misawa, H.; Healy, E. F.; Dewar, M. J. S. *J. Am. Chem. Soc.* **1987**, *109*, 6869.
(60) Kresge, A. J.; Perrin, C.; Schaad, L. Unpublished results.

Ab Initio Study of Rearrangement in 1-CH-1,2-$C_2B_{10}H_{11}$. Evaluation of the Cage Expansion Mechanism

Michael L. McKee

Contribution from the Department of Chemistry, Auburn University, Auburn, Alabama 36849.
Received January 13, 1992

Abstract: Two 13-vertex closo carboranes of molecular formula $C_3B_{10}H_{12}$ are calculated and compared to the carboranylcarbene, 1-CH-1,2-$C_2B_{10}H_{11}$, to determine the feasibility of an expanded cage mechanism in the degenerate rearrangement of the carbene. At the MP2/6-31G*//3-21G+ZPC level, an expanded cage is only 3.4 kcal/mol higher than the carbene, which suggests that the mechanism suggested by Jones is indeed possible. Calculations are also reported for the dianion *nido*-$C_2B_{10}H_{12}^{2-}$, which is related to the 13-vertex closo cage by removal of a C^{2+} vertex.

Introduction

As advances are made in carborane chemistry, it can be expected that rational synthetic routes will be developed for the formation of specific cages. One possible means is through cage expansion either by the condensation of coupled cages[1,2] or by the insertion of an exo substituent into a cage. Jones and co-workers[3-5] have explored the chemistry that results from the attachment of a carbene center to a carbon vertex of *o*-carborane. If the carbene is attached by a flexible tether, a bridge can form by insertion of the carbene into a C-H or B-H bond.[5] With a short tether, insertion into a C-H or B-H bond becomes more difficult, resulting in a strained three-membered ring when the carbene is directly attached to the carbon. An alternative pathway might be the insertion of the carbene directly into a boron-boron bond, thereby expanding the cage by one vertex.

The rearrangement of 2-methyl-*o*-carboranylcarbene (**1**) to 1-vinyl-*o*-carborane (**3**) as shown in eq 1 was observed by Jones and co-workers.[3] A possible mechanism would involve the intermediate **2** which would be expected to undergo 1,2 hydrogen migration to form the observed product **3**. While the intermediate **2** was not trapped, conversion of **1** → **3** by a pathway involving direct reaction of the carbene center with the methyl group was shown not to occur by ^{13}C labeling.[3] Noting that "it would be presumptuous to speculate too much in the absence of further experiments," Jones cautiously suggests[3] that the mechanism could involve a cage expansion induced by the divalent carbon to a 13-vertex cage. Interestingly, the analogous 2-methyl-*m*-

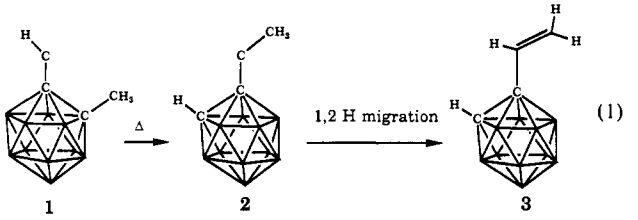

1 2 3 (1)

(1) (a) Corcoran, E. W.; Sneddon, L. G. *J. Am. Chem. Soc.* **1985**, *107*, 7446. (b) Corcoran, E. W.; Sneddon, L. G. In *Advances in Boron and the Boranes*; Liebman, J. F., Greenberg, A., Williams, R. E., Eds.; VCH: New York, 1988; pp 71-89 and references cited therein; Vol. 5 in the series Molecular Structure and Energetics.
(2) Grimes, R. N. In *Advances in Boron and the Boranes*; Liebman, J. F., Greenberg, A., Williams, R. E., Eds.; VCH: New York, 1988; pp 235-263; Vol. 5 in the series Molecular Structure and Energetics.
(3) Chari, S. L.; Chiang, S.-H.; Jones, M., Jr. *J. Am. Chem. Soc.* **1982**, *104*, 3138.
(4) L'Esperance, R. P.; Li, Z.-h.; Van Engen, D.; Jones, M., Jr. *Inorg. Chem.* **1989**, *28*, 1823.
(5) Wu, S.-h.; Jones, M., Jr. *Inorg. Chem.* **1986**, *25*, 4802.

0002-7863/92/1514-5856$03.00/0